WING LAMINAR BOUNDARY LAYER IN THE PRESENCE OF A PROPELLER SLIPSTREAM*

S.J. Miley and R.M. Howard
Texas A&M University
College Station, TX, USA

B.J. Holmes
NASA Langley Research Center
Hampton, VA, USA

ICAS-86-1.10.2

Abstract

The effects of a propeller slipstream on the wing laminar boundary layer are being investigated. Hot-wire velocity sensor measurements have been performed in flight and in a wind tunnel. It is shown that the boundary layer cycles between a laminar state and a turbulent state at the propeller blade passage rate. The cyclic length of the turbulent state increases with decreasing laminar stability. Analyses of the time varying velocity profiles show the turbulent state to lie in a transition region between fully laminar and fully turbulent. The observed cyclic boundary layer has characteristics similar to relaminarizing flow and laminar flow with external turbulence.

I. Introduction

It is becoming increasingly apparent the natural laminar flow (NLF) is a technology whose time has come to the general aviation industry. What had been the exclusive province of high performance sailplanes, is now commonplace in sport aircraft and is appearing on advanced technology prototype business aircraft. The adoption of NLF methodology brings numerous design problems in the general area of aerodynamic cleanliness. An important design problem for propeller driven aircraft is where to put the propeller slipstream. Tractor propeller installations offer many advantages. A generally accepted disadvantage, however, is that the propeller slipstream will come in contact with some parts of the airframe and eliminate the beneficial effects of laminar flow from the affected areas. The commonly applied solution is to adopt pusher installation designs to remove the slipstream from contact with the airframe. Pusher installations have their disadvantages also, however. Increased propeller vibration and nosie from wake cutting by the propeller blades is a common problem. In a recent survey of propeller propulsion integration technology by Miley and von Lavante[1], no clear advantage was found in the comparison of tractor versus pusher wing mounted installations. This conclusion is based upon a review of available published data from 1930 to the present. As part of the Viscous Drag Reduction Research Program at NASA Langley Research Center, Texas A&M University (TAMU) has been investigating the effects of the propeller slipstream on natural laminar flow.

Early observations of the effect of the propeller slipstream on boundary layer transition have not resulted in consistent conclusions. Young and Morris[2,3] and Hood and Gaydos[4] concluded from their investigations that the propeller slipstream caused the point of transition to move forward to a location near the leading edge. Reports by Zalovcik[5], and Zalovcik and Skoog[6] describe wing boundary layer measurements in propeller slipstreams performed on P-47 aircraft utilizing an NACA 230 series wing section and an NACA 66 series laminar flow wing section. Their results show little effect of the slipstream on transition for the NACA 230 section; however, the test with the NACA 66 series section resulted in the transition point location moving forward from 50 to 20 percent chord. The general consensus from this early work is that the propeller slipstream reduced the extent of laminar flow by forcing transition to occur earlier.

Recent work by Holmes, Obara and Yip[7] and Holmes, et al.[8] brings into question the validity of the ability of the early measurement methods to accurately determine transition. Time-dependent behavior, particularly at frequencies associated with propeller blade passage rate, was not measurable by techniques commonly employed at that time. Measurements by Holmes, et al.[8] using surface hot-wire sensors indicate the existence of a cyclic turbulent behavior resulting in convected regions of turbulent packets between which the boundary layer appears to remain laminar (Figure 1).

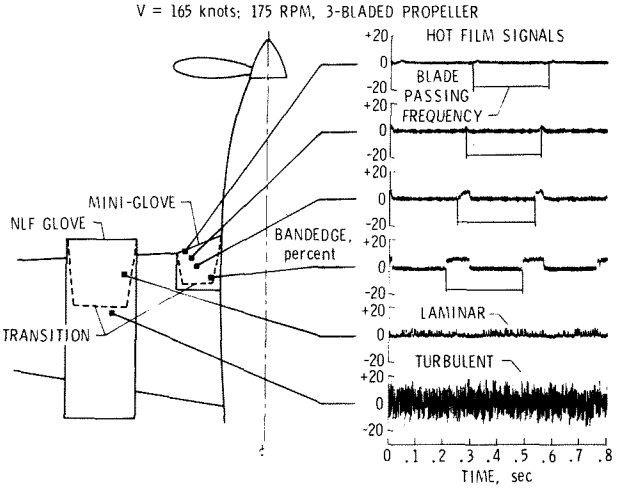

Figure 1. Surface hot-film measurements by Holmes et al. [7] showing cyclic laminar/turbulence behavior of boundary layer within propeller slipstream.

* This research is supported by NASA Langley Research Center Grant No. NAG 1-344.

II. Experimental Investigations

Flight Experiments

At Texas A&M University, flight measurements of the wing boundary layer in the slipstream have been made on a Gulfstream Aerospace GA-7 Cougar at two chord locations using a dual-probe hot-wire velocity sensing system. One probe was located adjacent to the surface well within the boundary layer and the other was located directly above in the external flow. The results of the flight test are shown in Figures 2-4.

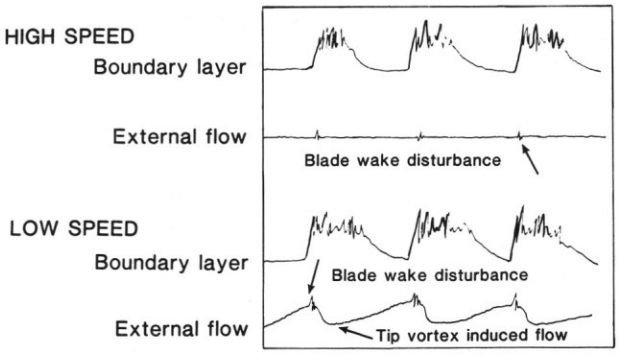

Figure 2. Identification of hot-wire velocity sensor signals in Figures 3-4.

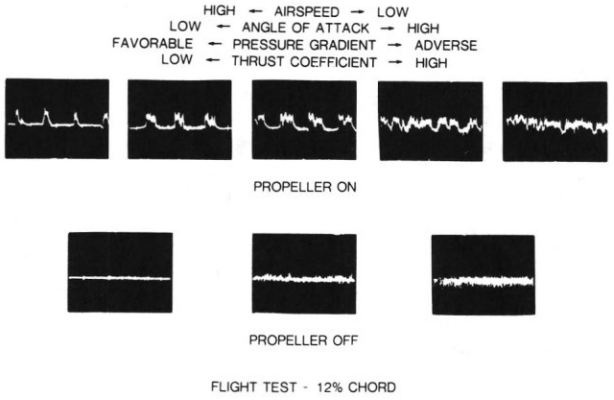

Figure 3. Velocity signal in boundary layer near surface, showing cyclic laminar/turbulent flow (propeller on) and laminar-transition-turbulence (propeller off).

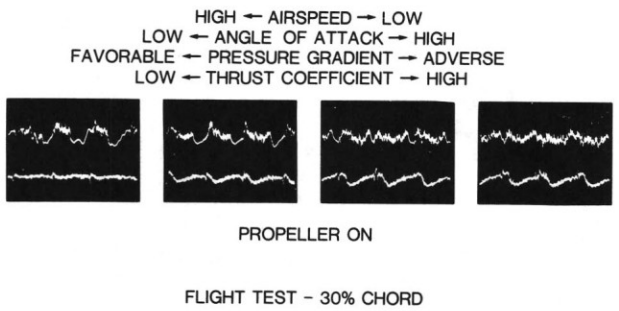

Figure 4. Velocity signals in boundary layer near surface and in external flow.

The signal traces are time histories of the local flow velocities in the boundary layer near the surface and in the external flow. The boundary layer velocity signal shows a periodic laminar/turbulent behavior. The change to turbulent flow results in an increase in the velocity seen by the probe because of the fuller turbulent profile. This change in profile results from periodic disturbances in the external flow due to the viscous wake shed from the propeller blade. The length of time which the cyclic turbulence remains in the boundary layer is dependent upon the laminar stability in the differing pressure gradients from the high-speed to the low-speed end. At the high-speed end, the pressure gradient is strongly favorable, and laminar stability is correspondingly high. Here, the boundary layer reverts almost immediately back to laminar flow after the passage of the external disturbance. At the low-speed end, the pressure gradient is no longer strongly favorable, laminar stability is greatly decreased, and the turbulence remains for almost the total cycle.

The effect of reduced laminar stability at the 30 percent chord location is evident in Figure 4. Here also is seen the character of the external flow disturbance due to the propeller slipstream. The viscous blade wake appears as a short wave impulse barely discernible at the high-speed end. As the speed is reduced, the propeller blade operates at an increasingly higher angle of attack and the viscous wake grows, leading to a more pronounced impulse disturbance signal. This is noted in the figures in terms of the propeller thrust coefficient. The low frequency wave pattern which develops in the external slipstream flow is due to the propeller tip vortex. As demonstrated by Sparks and Miley[9], the helical tip vortex induces an axial component in the slipstream velocity which increases with vortex strength (propeller thrust coefficient), and as the edge of the slipstream boundary is approached. While the tip vortex induced flow dominates the slipstream velocity signal, it will be shown that it is the relatively smaller blade viscous wake disturbance which is affecting the laminar boundary layer.

A slipstream disturbance flow model (Figure 5) was constructed from an analysis of the flight data. The viscous wake from the propeller blade forms a helical sheet which is split by the wing.

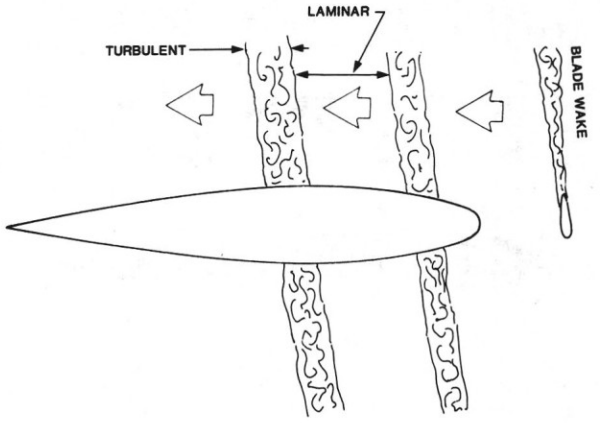

Figure 5. Slipstream disturbance flow model.

The turbulence in the helical wake is seen by a stationary point in the boundary layer as a periodic change in external flow turbulence. The laminar boundary layer responds by transitioning to the turbulent state and then returning to the laminar state through a reverse-transitional process based upon the degree of local laminar stability.

Wind Tunnel Investigation

A small-scale wind tunnel test program was begun to study the boundary layer response in more detail. The test model was a 30-inch chord NACA 0012 composite wing section with an 18-inch diameter single-bladed propeller and electric motor mounted at wing level at one-fifth chord distance upstream. Measurements were made at various angles of attack with a constant temperature hot-wire anemometer system and dual-probe configuration similar to that used in flight. The probes were traversed in a chordwise direction along the airfoil with the probe support free to pivot allowing the sensors to follow the airfoil contour. The probe heights above the surface were maintained at approximately 0.01 and 1.0 inches.

Two runs are shown in Figures 6-8. Figure 6 describes the signals seen in the photographs in the following figures. In each photograph the upper trace is the velocity in the boundary layer near the surface; the middle trace is the velocity for the external flow probe; and the lower trace is the trigger signal for the oscilloscope obtained from a magnetic proximity transducer sensing propeller blade passage.

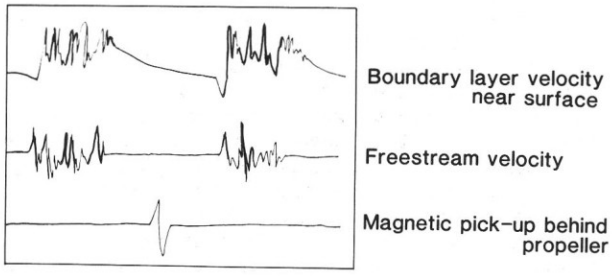

Figure 6. Identification of hot-wire velocity sensor signals in Figures 7-8.

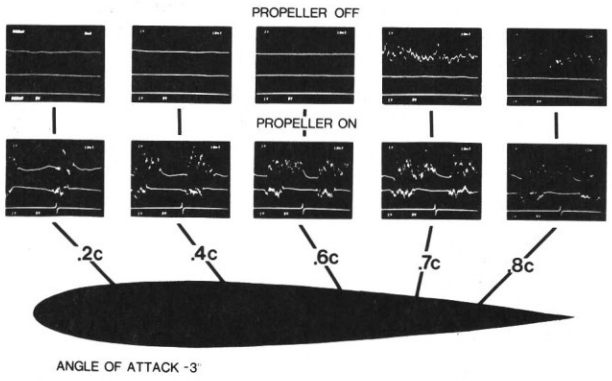

Figure 7. Velocity signals in boundary layer near surface and in external flow, showing cyclic laminar/turbulent flow (propeller on) and laminar-transition-turbulence (propeller off). -3° angle of attack.

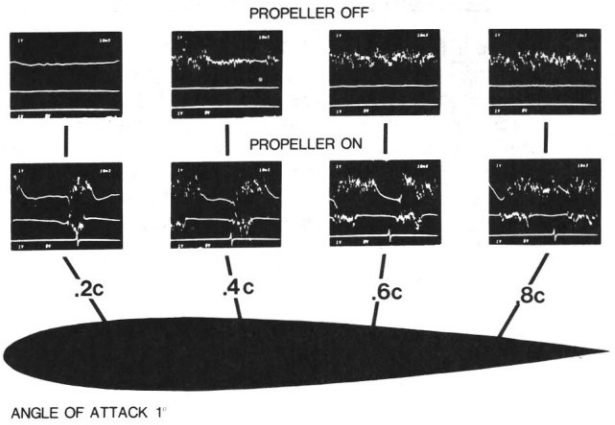

Figure 8. Velocity signals in boundary layer near surface and in external flow, showing cyclic laminar/turbulent flow (propeller on) and laminar-transition-turbulence (propeller off). +1° angle of attack.

Figure 7 shows a series of measurements at -3 degrees angle of attack resulting in a favorable pressure gradient along the upper surface. The upper row of photographs shows time histories of velocities at chord locations indicated with the propeller off. Transition takes place at approximately 70 percent chord at a chord Reynolds number of 6×10^5. Low frequency Tollmien-Schlichting waves appear with intermittent bursts of turbulence.

The lower row of photographs shows the velocities measured with the propeller running. The growth of the turbulent part of the cycle increases with decreasing laminar stability in the chordwise direction. Evident also is cyclic relaminarization of the previously turbulent region on the aft portion of the airfoil. Note this effect in the photograph for the 80 percent chord location. This behavior was seen in the flight data, but is more pronounced here, possibly due to the low Reynolds number. The waveform of the cyclic velocity variation can be noted, with the immediate jump to a turbulent velocity level with the arrival of the external disturbance. After the disturbance passes, the velocity returns to the laminar level as an exponential decay.

Figure 8 shows the results for 1 degree angle of attack. The pressure gradient is less favorable over the upper surface; the laminar boundary layer responds by transitioning now at 40 percent chord. More evident here is the cyclic relaminarization of the previously turbulent boundary layer. For the low test Reynolds number, the propeller slipstream appears to have a beneficial effect in the turbulent flow region of the airfoil. The mechanism behind the relaminarization is not understood at present. Possibilities include a reaction to the cyclic external flow turbulence and/or three-dimensional effects from the swirl component in the helical wake sheet.

A second series of experiments was conducted utilizing a single hot-wire probe to traverse the boundary layer normal to the surface. Runs were made at three angles of attack. The velocity time histories were digitized through a microcomputer and stored on floppy disk for analysis. Sufficient data were taken to construct time histories of the mean velocity profile, and of the turbulence intensity at each corresponding point within the profile. A representative plot of these data is given in Figure 9. The mean streamwise velocity across a blade wake passage cycle is plotted with the turbulence intensity superimposed as a "turbulence intensity envelope". Three positions across the boundary layer are displayed. The upper trace shows the external flow turbulent disturbance. There is a velocity defect, characteristic of momentum-loss wake profiles. The lower trace shows the response near the surface to be an increase to a turbulent velocity followed by a decay back to the laminar state, as has been seen previously. The turbulence intensity decreases with the reversion to laminar flow.

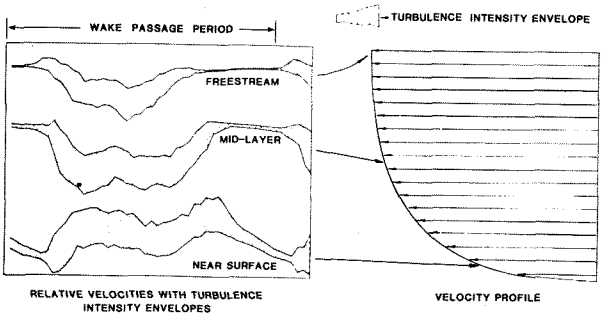

Figure 9. Time histories of the mean velocity and turbulence intensity at three vertical positions in the boundary layer. Data for one wake passage cycle.

III. Analysis and Results

Figure 10 shows three sets of velocity profiles, each set including three profiles at different points in the wake passage cycle. Each set represents a different angle of attack, giving pressure gradient effects ranging from favorable to adverse. The profiles were not normalized with respect to their individual thicknesses. Note that the bottom line does not represent the surface of the airfoil, but the lowest point in the boundary layer at which measurements could be taken. The profiles within each set are identified according to their position in the wake passage cycle, i.e. "laminar," "reverse-transitional," and "turbulent". Each of these positions also corresponds to a level of external flow turbulence intensity. The turbulence intensity distribution (profile) through the boundary layer for the 0 degree angle of attack case is shown in Figure 11. Due to limitations of the digitizer, the upper cut-off frequency of the data is approximately 100 hertz. Also, the wind tunnel has a low frequency surge which was not removed from the data. It is seen that there is a correspondence between the external flow turbulence intensity, the boundary layer velocity profile, and the boundary layer turbulence intensity profile.

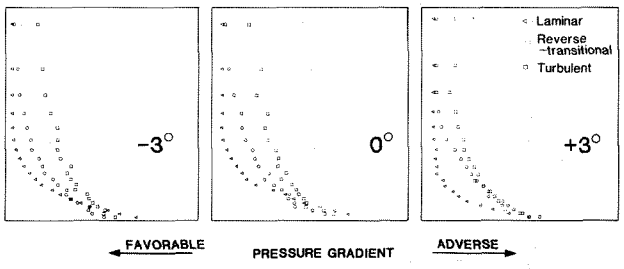

Figure 10. Boundary layer velocity profiles for three different angles of attack and for three different positions in the wake passage cycle.

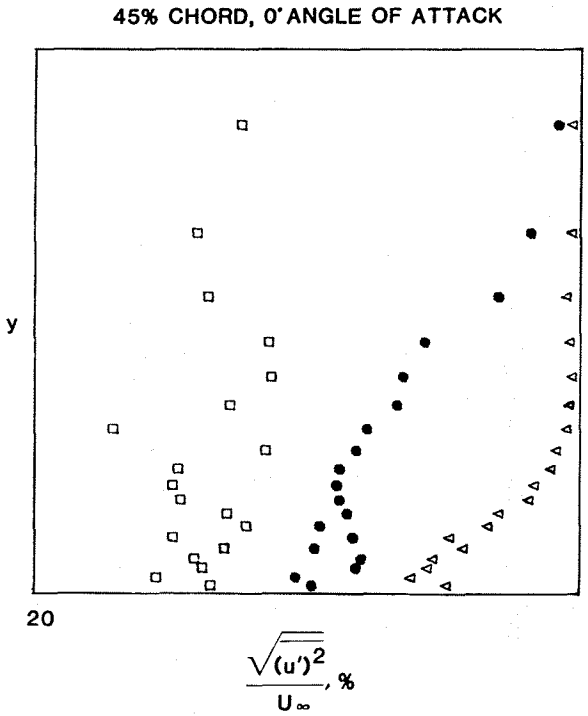

Figure 11. Turbulence intensity profiles for three different positions in the wake passage cycle. 0° angle of attack.

The effect of external flow turbulence on laminar and turbulent boundary layers has been investigated to a limited extent, primarily with concern to heat transfer. The work of Dyban, Epik and Surpun[10] is summarized in Figures 12-14. The laminar boundary layer over a flat plate is subjected to different levels of external flow turbulence intensity. The resulting boundary layer velocity and turbulence intensity profiles are shown in the figures. As the external flow turbulence intensity is increased, the velocity profile becomes fuller.

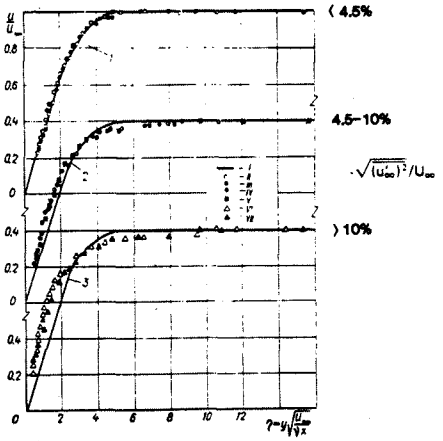

Figure 12. Boundary layer velocity profiles for three ranges of external flow turbulence. Blasius (flat plate) profile shown for reference. Dyban et al.[10].

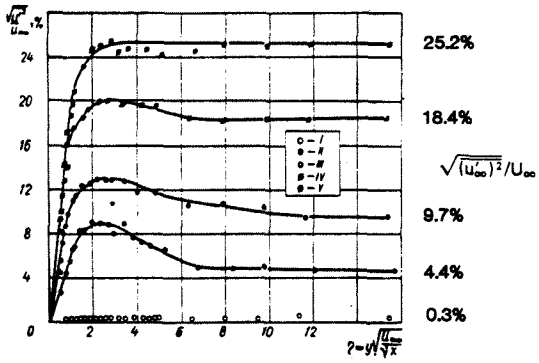

Figure 13. Boundary layer turbulence intensity profiles for different external flow turbulence intensity levels. Dyban et al.[10]

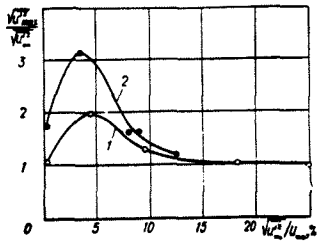

Figure 14. Ratio of boundary layer peak turbulence intensity to external flow turbulence intensity for two different Reynolds numbers. Dyban et al.[10]

Three distinct ranges of external turbulence intensity have been identified according to the respective generation of turbulence within the boundary layer. As shown in Figure 14, these ranges are: for an external turbulence intensity less than 4.5 percent, the generated turbulence intensity in the boundary layer increases at a faster rate than the external flow turbulence intensity, the generated intensity reaching peak levels 2 to 3 times as large depending on the Reynolds number; for 4.5 to 10 percent external flow turbulence intensity, the generated turbulence intensity in the boundary layer increases at a slower rate than the external flow turbulence intensity, reversing the trend in the first range; and for an external flow turbulence intensity greater than 10 percent, the rate of increase of generated turbulence intensity in the boundary layer monotonically approaches that of the external flow. The boundary layer velocity and turbulence intensity profiles in Figure 12 are identified respectively according to these ranges.

Comparison of the wind tunnel measurements with the the work of Dyban et al.[10] supports the view that the laminar boundary layer within the slipstream can be characterized as a boundary layer with a cyclic variation of external flow turbulence. As indicated in Figure 5, the source of the external flow turbulence is the viscous wake from the propeller blade. The passage of the wake over a point on the wing alters the laminar boundary layer according to the behavior shown in Figures 10-14. The increase in mean velocity shown in Figures 2-4 is the result of the change in the velocity profile. The length of the turbulence signal in Figures 2-4 is in part due to the change in the turbulence intensity profile. The available data show that near the surface, the turbulence will persist some time after the passage of the external turbulence. It is expected that the local pressure gradient will affect the rate of decay of the generated turbulence. This is presently being investigated. It is also important to note that with a definite turbulence profile within the boundary layer, a single point measurement by a hot-wire sensor can give misleading information. A thinner boundary layer would register a shorter turbulence time length than a thicker one because of the relative position of the sensor. With the present understanding, the model of Figure 5 has been updated, and the current model is shown in Figure 15. In this figure the relative thickness of the boundary layer and the persistence of the turbulence is emphasized.

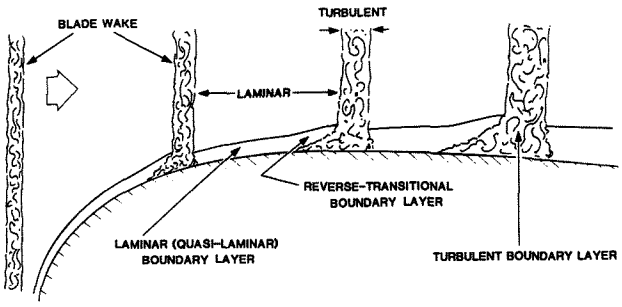

Figure 15. Current slipstream flow disturbance model, showing effect on laminar boundary layer.

An analysis was performed to determine where these external turbulence boundary layers lie in relation to conventional laminar and turbulent flows. Shape factor correlations between H_{12} and H_{32} were calculated from the wind tunnel data.

Data for each time step in the wake passage cycle were averaged over fifty cycles, smoothed, fit with a cubic spline and integrated for values of H_{12} and H_{32}. Figures 16-17 show the correlation across a wake passage cycle for an angle of attack of 0 degrees at chord locations of 15 and 45 percent, and for an angle of attack of 3 degrees at a chord location of 30 percent. Also included in the figures are the wake passage cycle time histories of the freestream mean velocity and turbulence intensity at the three chord positions. The curves plotted in the figure are the correlations utilized by Eppler[11] for laminar and turbulent flow as determined from similar solutions and empirical data.

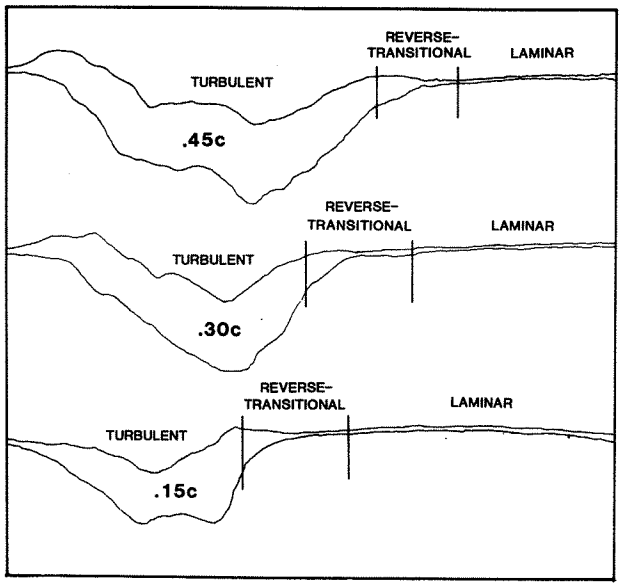

Figure 16. Time histories of external flow turbulence intensity.

In Figure 17 the time step data points corresponding to conditions where the boundary layer is indicated to be laminar lie on the laminar shape factor curve. The effect of the more adverse pressure gradient at 3 degrees angle of attack is seen by noting that the respective data points are shifted to lower vales of H_{32}. As the cycle is progressed, the velocity profile shifts to a highly stable form under the influence of the external turbulence, then reverts back to the conventional laminar range. In each case the shape factor correlation indicates that the boundary layer based on velocity profile behavior never attains the predicted turbulent relationship. In Figures 18-20, shape factors determined from the external turbulence flow boundary layer velocity profiles of Dyban et al.[10] and from relaminarization flow boundary layer velocity velocity profiles of reference (12) are plotted with the laminar and turbulent correlation curves. The external turbulence shape parameter values follow that same path as the slipstream results. The relaminarizing flow shape parameter values initially move in the direction of a newer (younger) turbulent boundary layer, then loop back and proceed in the direction of the laminar curve. The relaminarizing boundary layer is initially turbulent. Under the action of a

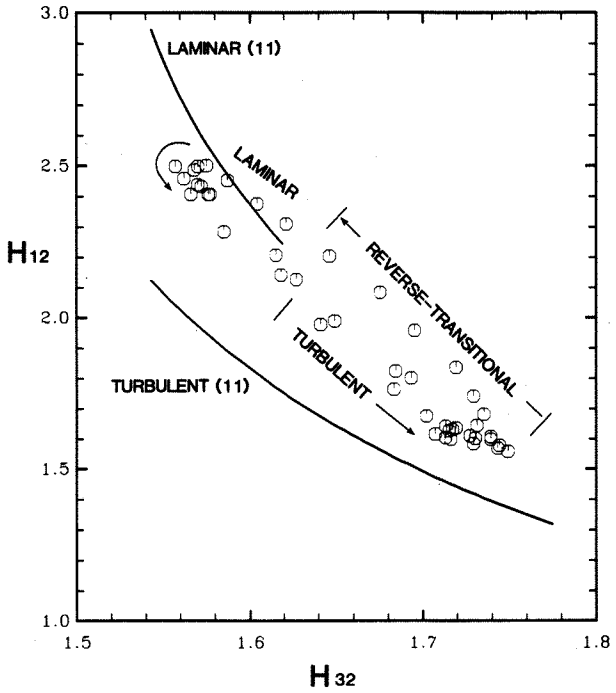

Figure 17. Shape factor variation for 15 percent chord. 0° angle of attack.

strongly favorable pressure gradient, a reversion to a laminar-like state takes place. The progress of the relaminarization in relation to the laminar and turbulent curves is noted in the figure. The turbulence intensity profiles of the relaminarizing flow from reference (12) are given in Figure 21. The profiles are similar to those of the external flow turbulence boundary layers.

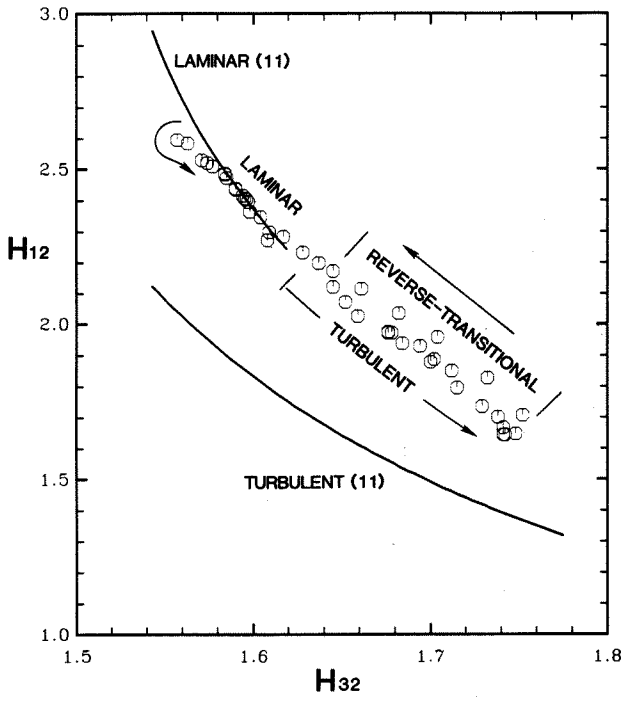

Figure 18. Shape factor variation for 45 percent chord. 0° angle of attack.

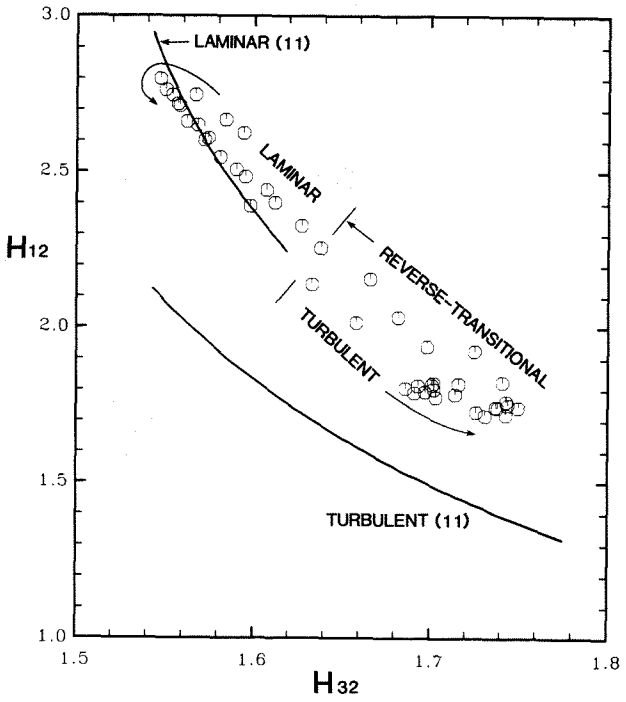

Figure 19. Shape factor variation for 30 percent chord. +3° angle of attack.

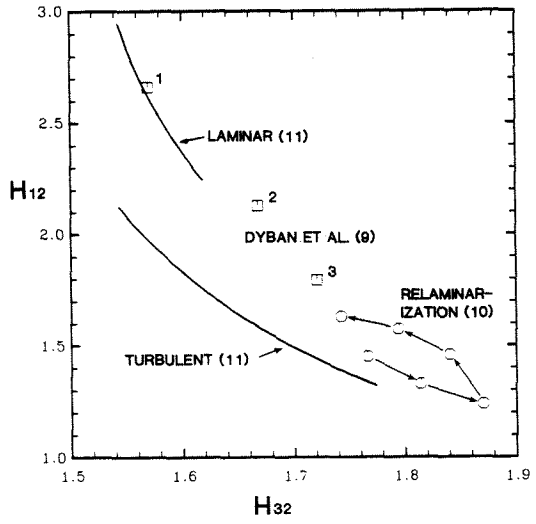

Figure 20. Boundary layer shape factor variation for external flow turbulence of Dyban et al.[10] and for relaminarizing flow (reference 12).

The results in Figures 16-20 raise the question of a class of boundary layers which lie between the fully laminar and fully turbulent states. In the case of the external turbulence flows, the terms "pseudo-laminar" and "pseudo-turbulent" have been used. In consideration of where they lie in terms of shape parameter values, the term "transitional" may be more appropriate. The implication of the data in the figures is that a "transitional" shape factor correlation curve may exist which connects laminar and turbulent flows. This concept will

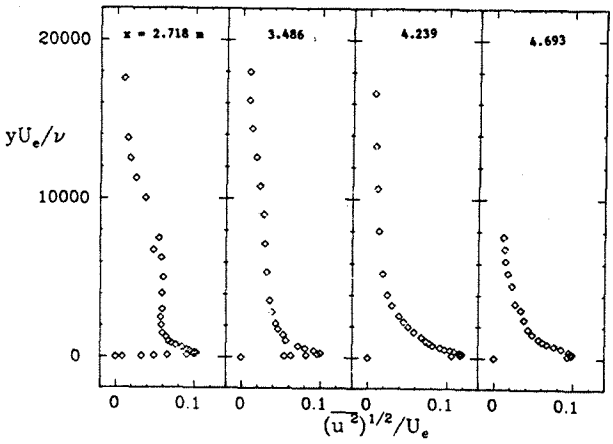

Figure 21. Boundary layer turbulence intensity profiles for relaminarizing flow (reference 12). Increasing values of x denote downstream progress towards relaminarization.

be investigated in the effort to develop a practical boundary layer prediction method for the slipstream case.

IV. Summary

The laminar boundary layer within a propeller slipstream is affected by the viscous wake from the propeller blade. The wake forms a helical sheet which is split by the wing and passes over the upper and lower surfaces. Across a propeller blade wake passage cycle, the boundary layer at a point on the airfoil surface goes through the distinct phases of turbulent, reverse-transitional and laminar behavior consistent with a cyclic variation in external flow turbulence. The turbulent phase is characteristic of boundary layer flow with external turbulence, and exhibits velocity profiles which lie in a transitional region between fully laminar and fully turbulent flow. The cyclic external turbulence may also influence the turbulent boundary layer in such a way as to cause periodic relaminarization as has been observed in flight and in the wind tunnel.

V. References

1. Miley, S.J. and von Lavante, E., "Propeller Propulsion Integration - State of Technology Survey," NASA CR

2. Young, A.D. and Morris, D.E., "Note on Flight Tests on the Effect of Slipstream on Boundary Layer Flow," R&M No. 1957, Brit. A.R.C., 1939.

3. Young, A.D. and Morris, D.E., "Further Note on Flight Tests on the Effect of Slipstream on Boundary-Layer Flow," RAE Rep. No. B.A. 1404b, 1939.

4. Hood, M.J. and Gaydos, M.E., "Effects of Propellers and Vibration on the Extent of Laminar Flow on the NACA 27-212 Airfoil," NACA ACR (WR L-784), 1939.

5. Zalovcik, J.A., "Flight Investigation of the Boundary Layer and Profile Drag Characteristics of Smooth Wing Sections on a P-47D Airplane," NACA WR L-86, 1945.

6. Zalovcik, J.A., and Skoog, R.B., "Flight Investigation of Boundary Layer Transition and Profile Drag of an Experimental Low-Drag Wing Installed on a Fighter-Type Airplane," NACA WR L-94, 1945.

7. Holmes, B.J., Obara, C.J., and Yip, L.P., "Natural Laminar Flow Experiments on Modern Airplane Surfaces," NASA TP 2256, 1984.

8. Holmes, B.J., Obara, C.J., Gregorek, G.M., Hoffman, M.J., and Freuhler, R.J., "Flight Investigation of Natural Laminar Flow on the Bellanca Skyrocket II," SAE Paper 830717, 1983.

9. Sparks, S.P. and Miley, S.J., "Development of a Propeller Afterbody Analysis with Contracting Slipstream," SAE Technical Paper Series 830743, April 1983.

10. Dyban, Ye.P., Epik, E.Ya., and Surpun, T.T., "Characteristics of the Laminar Boundary Layer in the Presence of Elevated Free-Stream Turbulence," Fluid Mechanics - Soviet Research, Vol. 5, No. 4, July-August 1976, pp. 30-36.

11. Kline, S.J., Cantwell, B.J. and Lilley, G.M., ed. "The 1980-81 AFSOR-HTTM-Stanford Conference on Complex Turbulent Flows: Comparison of Computation and Experiment," Thermosciences Division, Mechanical Engineering Department, Stanford University, 1981.

12. Eppler, R. and Somers, D.M., "A Computer Program for the Design and Analysis of Low-Speed Airfoils," NASA TM 80210, 1980.